Transport and retention of n-hexadecane in cadmium-/naphthalene-contaminated calcareous soil sampled in a karst area

Yiting Huang
School of Civil Engineering and Architecture, Guangxi University
Yankui Tang (cindyyktang@gxu.edu.cn)
School of Resources, Environment and Materials, Guangxi University
Yi Liang
School of Resources, Environment and Materials, Guangxi University
Zhenze Xie
School of Resources, Environment and Materials, Guangxi University
Jipeng Wu
School of Resources, Environment and Materials, Guangxi University
Jiajie Huang
School of Resources, Environment and Materials, Guangxi University
Shanxiong Wei
School of Resources, Environment and Materials, Guangxi University
Shaojiang Nie
School of Resources, Environment and Materials, Guangxi University
Tao Jiang
School of Resources, Environment and Materials, Guangxi University

Research Article

Keywords: N-hexadecane, Freundlich, pH, Column experiments, Flow velocity, Hydus-1D

Posted Date: September 6th, 2022

DOI: https://doi.org/10.21203/rs.3.rs-2006218/v1

Additional Declarations: No competing interests reported.

Version of Record: A version of this preprint was published at Environmental Geochemistry and Health on June 26th, 2023. See the published version at https://doi.org/10.1007/s10653-023-01664-y.

Abstract

Petroleum hydrocarbon pollutants in karst areas have aroused widespread concern due to their toxicity. It is crucial to gain knowledge on transport and retention of petroleum hydrocarbons in karst areas. Calcareous soils in karst areas were contaminated by cadmium/naphthalene due to the industrial and agricultural activities, however, the fates of petroleum hydrocarbons in these contaminated calcareous soils have been rarely studied. In this study, n-hexadecane was selected as a model petroleum hydrocarbon. Batch experiments were conducted to explore the adsorption behavior of n-hexadecane on cadmium-/naphthalene-contaminated calcareous soils at various pH, and column experiments were performed to investigate the transport and retention of n-hexadecane under various flow velocity. The results showed that Freundlich model can well describe the adsorption behavior of n-hexadecane on all samples (R^2>0.9). According to the adsorption coefficient (K_f), the presence of cadmium/naphthalene dramatically increased the adsorption efficiency of n-hexadecane on calcareous soils, and the increasing pH value reduced the adsorption capacity in all groups. The transport of n-hexadecane in all samples were well described by two kinetic sites model of Hydrus-1D with R^2>0.9. The higher effluent concentration of n-hexadecane indicates that n-hexadecane can more effectively break through the cadmium-/naphthalene-contaminated calcareous soil with high flow velocity, which means the lower n-hexadecane retention in this situation. The observation can be explained by the electrostatic repulsion between n-hexadecane and each soil sample. These findings have important implications for the government of groundwater in calcareous soils from karst areas.

Introduction

Petroleum hydrocarbons are inevitably released into soils by the spill and leakage from tanks at petrol stations and industrial sites, then they transport downward along the soil layer and enter groundwater. The extensive and long-term petroleum hydrocarbons pollutants pose a threat such as carcinogenic, teratogenesis, and gene mutations to public health through the food chain (Wu et al., 2017). Some works have found that the fate of petroleum hydrocarbons may definitely influence the remediation efficiency (Ossai et al., 2020). N-hexadecane, a hydrophobicity fraction represents the ignitability of diesel fuel, has been usually chosen as the model petroleum hydrocarbon by many researchers to study on the environmental risks and the remediation (Brils et al., 2002; Samaei et al., 2020; Samaei et al., 2022). Thus, to better select the treatment option for remediation, it is necessary to investigate the transport and retention of n-hexadecane in soil environments.

To date, the transport and retention of petroleum hydrocarbons in soils have been studied. Transport of petroleum hydrocarbons in quartz sand is promoted by increasing pH due to the increasing electrostatic repulsion between contaminations and particle surfaces (Wang et al., 2020b). Ca^{2+} provides the adsorption sites of petroleum, thus elevated concentration of Ca^{2+} can increase the retention of petroleum in soil (Luo et al., 2022; Zhang et al., 2012). The high-speed and short-term infiltration of petroleum hydrocarbons into deeper soil layers are also affected by the minimum content of clay and the

lower ionic strength (Rosales et al., 2014; Wang et al., 2020b). Furthermore, the stronger leaching as torrential rain and flood changes the release of petroleum hydrocarbons in soil (Dror et al., 2002). In fact, one serious challenge impacting the soil remediation of n-hexadecane is the presence of other contaminations. Contaminated natural soils with n-hexadecane at petrol stations and industrial sites have been usually found heavy metals or Polycyclic Aromatic Hydrocarbons (PAHs), and the mixture may bring more risk to public health (Khudur et al., 2018; Li et al., 2021). Heavy metals cause long-term pollution in soils due to the lower bioavailability (Jampasri et al., 2016). PAHs, the toxic compounds in diesel oil and crude oil with uniquely stable structures, still retain in soils for a long time after n-hexadecane have been degraded (Zhou et al., 2019). Moreover, heavy metals change the organic matter, water holding capacity and pH value of soils (Zhao et al., 2017; Zheng et al., 2016). Besides, hydrophobic PAHs change the properties of soils by covering with a thin insulating film (Steliga and Kluk, 2020), lowering porosity, increasing resistance to penetration, aggregating particles in plaques, etc (He et al., 2013; Li et al., 2012; Wu et al., 2013). However, the influence of heavy metals/PAHs in soils on n-hexadecane transport has been overlooked by previous studies.

The presence of dissolution fissures, crevices, and channels in karst areas cause stronger interaction between surface water and groundwater (Yang et al., 2019). As a result, the groundwater is more easily to be contaminated in karst areas than in non-karst areas (Lü et al., 2020). Thus, it is necessary to pay more attention to the process of how petroleum hydrocarbons in soil enter groundwater, since calcareous soils in karst areas have been seriously contaminated by petroleum hydrocarbons (Guo et al., 2020; Peng et al., 2022). Moreover, as an stability derivative of PAHs (Chen et al., 2009; Xu et al., 2022), naphthalene has effectively retained in karst areas by abundant soil organic matter (SOM) (Sun et al., 2019). Higher abnormal enrichment of cadmium (Cd) in karst than in non-karst due to the natural weathering of carbonate rock, the higher pH value, and the increasing soil organic carbon (SOC) (Albert et al., 2021; Wen et al., 2020). Therefore, three types of calcareous soil samples (origin calcareous soil, Cd-contaminated calcareous soil and naphthalene-contaminated calcareous soil) were chosen for studying the transport and retention of n-hexadecane due to their different properties. The objectives of this study are to (1) reveal the effect of Cd/naphthalene and pH on n-hexadecane adsorption, (2) investigate the effect of Cd/naphthalene and flow velocity on the transport and retention of n-hexadecane, and (3) explore the mechanisms governing the transport of n-hexadecane in vertical direction of Cd-/naphthalene-contaminated calcareous soil. The results can contribute to the development of palliative measures and management strategies to reduce the risks of environmental health.

Methods And Materials

Reagents

N-hexadecane and naphthalene were obtained from Shanghai Macklin Biochemical Co., Ltd with a purity > 98%. Cadmium chloride was purchase from Tianjin Kermel Chemical Reagent Co., Ltd. KCl was purchased from Sinopharm Chemical Reagent Co., Ltd, Shanghai, China. Methanol, acetone, and n-hexane were supplied by T. JKE MAO Chemical Reagents CO., LTD. In this study, all reagents were at least

analytical reagent, and all solutions were prepared using Mlilli-Q water (resistance of 18.2 MΩ.cm at 25℃).

Preparation and characterization of calcareous soil samples

Calcareous soil samples were collected at the 0–20 cm below the ground surface from Fusui, Guangxi Zhuang Autonomous Region, China (22°56'43.6"N, 107°15'46.7"E). Calcareous soil samples were air dried at room temperature (25 ± 1℃) for one week, and they were sieved through a 2-mm mesh before experiments. The physical and chemical properties of the soil samples were provided in supplementary materials (Table S1). Table S1 presented that the background concentration of Cd in collected calcareous soils was below the detection limit of standard from China. N-hexadecane and naphthalene are not detected. According to Soil Environmental Quality Risk Control Standard for Soil Contamination of Development Land in China (risk screening values for soil contamination), the concentration of Cd and naphthalene was configured to be 20 mg/kg and 70 mg/kg in tested conditions, respectively. After soil samples and contamination solution were evenly mixed, the mixtures were placed in a fume hood for 90 days. The origin calcareous soil, Cd-contaminated calcareous soil and naphthalene-contaminated calcareous soil were marked as OS, CS and NS, respectively.

Fourier transform infrared spectroscopy (FTIR, IRTracer-100, Shimadzu, Japan) was used to examine functional group in freeze-dried soil samples at wave numbers from 400 to 4000 cm^{-1}. X-ray diffraction (D8 Dicover, Bruker Axs Gmbh, Germany) was used to analyze the crystalline constituents of freeze-dried soil samples. The concentration of dissolved organic matter (DOM) was detected by TOC-VCPH (Shimadzu, Japan). The zeta potential was measured by Nanobrook Ommi, Brookhaven (America). The fluorescence spectrometer (F-7000, Hitachi, Japan) was used to measure the three-dimensional excitation-emission matrix spectroscopy (3D-EEM) under the flowing conditions: excitation wavelengths of 200–450 nm (every 5 nm), emission wavelengths of 250–600 nm (every 1 nm), scan speed of 12000 nm/min, the excitation slit of 5 nm and emission slit of 5 nm.

Batch experiments

Before batch experiment, 0.5, 1.0 and 2.0 g soil samples were respectively mixed with 50 mL of 100 mg/L n-hexadecane solution into 100 mL conical flasks, and the mixtures were shaken for 12 h at 140 rpm and 25 ± 1 ℃. The ratio of soil samples to solution was selected 1.0 g for the stability of n-hexadecane quantification in batch experiments. In adsorption kinetic experiments, all conical flasks with parafilm (PM996, America) were shaken at various time scales (0.25, 0.5, 1, 2.5, 4, 8 and 12 h) in dark under the conditions of 140 rpm and 25 ± 1 ℃. In desorption kinetic experiments, the residues of preliminary adsorption kinetic experiments were mixed with 50 mL solution without n-hexadecane, and the mixtures was shaken at the same conditions as adsorption kinetic experiments. In adsorption isotherm experiments, 1.0 g soil sample was transferred to 50 mL various concentrations of n-hexadecane solution (50, 60, 80, 90 and 100 mg/L), and then the mixture was shaken at 140 rpm (25 ± 1 ℃) in dark for the

equilibrium time, respectively. Moreover, the pH was adjusted with value of 5, 7, 9 using 0.1 mol/L HCl or NaOH for investigating the effect of pH on n-hexadecane adsorption behavior by isotherm experiments.

All supernatants were collected after the mixtures were centrifuged at speed of 8000 rpm for 10 min. All the experiments were determined in triplicate using the standard experiment, and the concentration of n-hexadecane in liquid phase was detected by UV spectrophotometer (Shimadzu, Japan) at 257 nm.

Column experiments

The soil sample was wet-packed into a cylindrical column (3 cm inner diameter × 12 cm length). The schematic of experimental setup for column experiment is shown in Fig. S1. A peristaltic pump was used to pump influents from the bottom into column. The packed column was firstly saturated with background solution (1 mM KCl solution, which was used to minimize any volatilization loss (Rosales et al., 2014)) with the set velocity (1, 2, and 4 mL/min) for 3 h pre-equilibration and air-removing. After that, 2.0 pore volumes (PVs) tracer (5 mM KCl solution) was injected into the column, and then several PVs of background solution was not stopped injecting until tracer was monitored to be zero. The tracer was measured by Conductivity Meter (DDSJ-308A, Shanghai INESA Scientific Instruments Co., Ltd, China). Breakthrough curves (BTCs) of tracer were used to determine longitudinal dispersion coefficient (cm^2/min) in a column. Fig. S2 showed the BTCs of tracer can be well fitted with $R^2 > 0.99$ by STANMOD software, and a high degree of symmetry in column. The BTCs peak of tracer nearly reached the inlet concentration (the ratio was 93.6%), suggesting that KCl was a non-reactive tracer in this work. The following step was, 2.0 PVs of n-hexadecane solution (100 mg/L) with background solution was pumped into column, and then the column was flushed by several PVs of background solution. The effluents of n-hexadecane were determined by UV spectrophotometer (Shimadzu, Japan) at 257 nm. The BTCs of n-hexadecane were expressed as relative concentration (C/C_0) versus PV, where C and C_0 were the concertation of n-hexadecane in the effluents and influents, respectively. The BTCs of n-hexadecane were fitted by Hydrus-1D, and the details of this model were described by (Simunek et al., 1999). Moreover, two groups were set to assure the consistency the reproducibility of column experiment.

To better know the residue of n-hexadecane in a column, the packed column was excavated in 12 layers (from top to bottom) after column experiment was finished, and each layer was determined by Ultrasonic Extraction and Gas Chromatograph (GC, Shimadzu GC-2010, Japan). The parameter of GC system was referred by Determination of Extractable Petroleum Hydrocarbons (C10-C40) in China (HJ 894–2017).

Results And Discussion

Properties of soil sample

The FTIR spectrum of OS, CS and NS is given in Fig. 1. The transmittance peak at 3443 cm^{-1}, 1636 cm^{-1} and 1034 cm^{-1} represent the stretching of -OH, C=C / C=O and Si-O-Si, respectively. The XRD pattern of OS, CS and NS (Fig. 2) showed that all soil samples were composed of saponite, kaolinite, rodolicoite and

vanadium oxide. The FTIR spectrum and XRD pattern of OS, CS and NS indicated that the coating of Cd/naphthalene did not change the surface functional group and the mineralogical composition of calcareous soils. Table 1 is the zeta potential of OS, CS and NS. The OS, CS and NS are all negatively charged in the condition of this work, and the presence of n-hexadecane increased the negative surface potentials of OS, CS and NS since surface coating by hydrophobic compounds can change the zeta potential of porous media (Song et al., 2011; Yang et al., 2017b).

Table 1 The zeta potential of all soil samples

concentration of n-hexadecane	Zeta potentials (mV)		
	CS	OS	NS
0 mg/L	-15.84	-20.76	-23.03
100 mg/L	-29.11	-23.47	-24.63

The DOM concentration of CS (313.10 mg/kg) and NS (331.30 mg/kg) was higher than that of OS (88.35 mg/kg) (Table S1), suggesting that microbial communities in calcareous soil may respond to Cd/naphthalene (Schwarz et al., 2011; Wang et al., 2020a). DOM may control the fate of n-hexadecane in calcareous soil due to its amphipathic molecules. Fluorescence spectra of OS, CS and NS (Fig. 3) showed the intensity of tyrosine-like fluorescent peak in CS/NS were more significant than in OS, suggesting that CS/NS have more aromatic ring amino acids (Yan et al., 2019). The intensity of tryptophan-like fluorescent peak in CS/OS was stronger than in NS. Fulvic acid relates to the carbonyl and carboxyl groups, and it can increase the solubility of hydrocarbon (Lu et al., 2013). Clearly, the intensity of fulvic acid peak in CS was greater than in OS/NS. Fluorescence components of DOM in OS, CS and NS were shown in Fig. 4. It can be seen that the humic acid content of NS was smaller than that of OS/CS. It may result in the greater adsorption capacity of NS since the humic acid can generally inhibit the adsorption of hydrocarbon on porous media (Wang et al., 2017).

Adsorption and desorption kinetic of hexadecane on calcareous soil samples

N-hexadecane may be firstly trapped in calcareous soil through molecular adsorption, and later desorption may constitute the rate determining step. All samples were fitted well by the pseudo-first-order dynamics model with R^2> 0.9 (Fig. S3 and Table S2). Adsorption equilibrium time for n-hexadecane on OS, CS and NS were all 4 h, suggesting that the presence of Cd/naphthalene cannot change the adsorption equilibrium time. It may be causing by the homologous properties of calcareous soil samples (Yang et al., 2013). The adsorption rate constant (k_1) of OS was higher than that of CS/NS, which means Cd/naphthalene can increase the adsorption efficiency of n-hexadecane on calcareous soils. Desorption equilibrium time for n-hexadecane on OS, CS and NS were all 1 h, indicating that Cd/naphthalene cannot change the desorption equilibrium time. The k_1 of n-hexadecane adsorption on OS was lower than CS/NS

(Table S2), which means Cd/naphthalene can reduce the desorption efficiency of n-hexadecane on calcareous soils. In all cases, adsorption efficiency was higher than desorption efficiency, suggesting the desorption behavior of n-hexadecane cannot greatly influence the adsorption behavior in this work. On the whole, Cd/naphthalene can improve the adsorption capacity and decrease the desorption capacity of n-hexadecane on calcareous soils, but they cannot change the equilibrium time.

Effect of pH on the adsorption isotherm of n-hexadecane on the calcareous soil samples

In most cases, Freundlich (Fig. 5 and Table 2) is better than Langmuir (Fig. S4 and Table S3), which means the adsorption behavior of n-hexadecane on soil samples may not dependent on monolayer adsorption. In Table 2, K_f value (at pH=7) of n-hexadecane adsorption on soil samples was lower than that of on loess soil (Jiang et al., 2016) and modified diatomite (Xu et al., 2020). It can be summarized that Cd/naphthalene cannot obviously improve the adsorption efficiency of n-hexadecane on calcareous soils in comparison with other soils. At pH=7, K_f value of OS was lower than that of CS/NS, suggesting that Cd/naphthalene can improve the higher n-hexadecane adsorption capacity on calcareous soil. Previous studies have also found that adding metals can increase the adsorption of hydrocarbon on porous medias (Saeedi et al., 2018). Cd-coating porous medias can enhance the adsorption of anionic and neutral hydrocarbon compounds since the polar functional group in porous media was complexation with Cd (Wang et al., 2017). However, in this study, the surface functional group in calcareous soils did not change after Cd/naphthalene coating, therefore the improved adsorption efficiency may not absolutely depend on function group's change. Furthermore, the aggregation and hydrophobicity of porous media causing by Cd-coating can increase the adsorption efficiency of hydrocarbons (Nguyen et al., 2013). The negative charge of porous media surface can be shielded after coating naphthalene (Yang et al., 2017a), therefore the adsorption of n-hexadecane was inhibited. Moreover, the n value of all cases was lower than 1, indicating that adsorption sites in the surface of all soil samples (OS, CS and NS) were limitation although Cd/naphthalene can open more adsorption sites for n-hexadecane.

Table 2 The parameters of Freundlich

Soil sample	pH	K_f[a]	$1/n$[b]	R^2
OS	5	0.10±0.15	2.30±0.26	0.95
	7	0.00±0.01	2.10±0.36	0.98
	9	0.02±0.03	2.76±0.32	0.98
CS	5	0.26±0.38	1.89±0.33	0.95
	7	0.05±0.08	2.27±0.42	0.95
	9	0.01±0.02	2.48±0.25	0.98
NS	5	1.27±1.40	1.56±0.25	0.95
	7	0.82±0.82	1.65±0.22	0.96
	9	0.06±0.09	2.17±0.30	0.95

[a] K_f is the coefficient of Freundlich which positively associated with adsorption capacity.

[b] n is the sorption intensity.

In recent years, rainwater with higher pH value (pH=8.0) was found in a typical karst area (Zeng et al., 2020). Furthermore, previous studies have found that the adsorption of diesel oil on loess soil was weakened by increasing pH (Jiang et al., 2016) since pH improve the dissolution and dispersion of diesel oil (Delle Site, 2001; Pradubmook et al., 2003). However, the adsorption of naphthalene on biochar colloid had almost no effected by pH (Yang et al., 2017b) due to the little dissociation degree of nonpolar hydrocarbons in polar solution (Grządka, 2011). Therefore, the potential influence of pH on the n-hexadecane adsorption was investigated in this study. As shown in Fig. 5 and Table 2, it can be observed that the elevated pH (from 5 to 9) caused decreasing adsorption efficiency of n-hexadecane on OS, CS and NS. In this study, pH value was set from 5 to 9, thus the adsorption of n-hexadecane on each soil sample at pH=5 was the maximum. The adsorption of n-hexadecane on OS was weaker than CS/NS at pH=5 and pH=7. The K_f value of OS was higher than CS in alkaline environment (at pH=9). The n-hexadecane adsorption on NS remained stable from 5 to 7, but it was changed from pH=7 to pH=9. Some studies reported that the release of Cd/naphthalene in soils depended on pH since the bonds between contaminations and soils were broken by pH (Kicińska et al., 2022; Yang et al., 2001). Furthermore, the release of Cd/naphthalene in soils may open more adsorption sites for n-hexadecane. Moreover, the presence of impurities in n-hexadecane, such as long-chain carboxylic acids (Fang et al., 2015), and the unbalanced hydrophobic/hydrophilic properties at oil/water boundary in solution (Li and Bhushan, 2015) may influence the adsorption of hydroxyl ions (OH^-), thus n-hexadecane carries negative surface charge. The electronic mobility of the n-hexadecane and the adsorption sites on soil samples may change along with the increasing pH at aqueous phase (Kim et al., 2012; Li and Bhushan, 2015). Therefore, pH can influence the adsorption behavior of n-hexadecane on soil samples.

Effect of flow velocity on transport of n-hexadecane in the calcareous soil samples

The BTCs of n-hexadecane in the calcareous soil samples with the addition of various flow velocity are presented in Fig. 6. As shown in Fig. 6, all BTCs were symmetric in shape, implying that there was the physical equilibrium transport in column. The maximum value of C/C_0 were 28 %, 35 % and 48 % in OS, CS and NS with the set flow velocity of 1 mL/min, respectively, suggesting n-hexadecane may more effectively breakthrough the column of CS/NS than that of OS. Similarly, the maximum value of C/C_0 in CS/NS was higher than in OS at the set flow velocity of 2 and 4 mL/min. The two kinetic sites model of Hydrus-1D well described the BTCs of n-hexadecane in each soil sample with different Darcy velocity according to the higher correlation coefficient (R^2) between observed and simulated data (Table 3). The characteristic of BTCs for n-hexadecane in all soil sample column can be reflected by S_{max} and K_{att} of Hydrus-1D (Table 3). In all case, the S_{max} value of OS was higher than that of CS/NS, which means greater irreversible retention of n-hexadecane in OS. The greater value of K_{att} for CS/NS at all Darcy velocity reflects a rapid release process of n-hexadecane. The mass recovery rate of n-hexadecane in effluent are showed in Table 3. There is a higher mass recovery rate for n-hexadecane in the effluent of CS/NS packed column than that of OS packed column. On the whole, the transport of n-hexadecane in soil samples followed the order of CS/NS > OS at the same Darcy velocity, which means Cd/naphthalene can improve the transport efficiency of n-hexadecane. In Table 2, negative charge density of CS/NS was more than that of OS. The more negative charge of soil samples, the stronger electrostatic repulsions between the soil samples and the negatively charged n-hexadecane were, which is likely responsible for promoting the transport of n-hexadecane in CS/NS packed column (Wu et al., 2020). Furthermore, although naphthalene-coating cannot dramatically change the surface negative charge of calcareous soils, nonpolar naphthalene can lead to charge-shielding (Yang et al., 2017b).

The previous studies have proved that the transport of petroleum hydrocarbons with negative charge were inhibited by the decreasing pH due to the reduction in electrostatic repulsion (Cai et al., 2017; Wang et al., 2020b). Our previous batch experiments also showed that the electronic mobility of the n-hexadecane increased along with the increasing pH at aqueous system (Fig. 5 and Table 2). Moreover, the unique hydrological and geological structures in karst areas lead to variable flow velocity, and pollutants are more easily to rapidly transport in the pipeline systems of karst (Jiang et al., 2018). Therefore, this section only investigated the potential influence of flow velocity on the n-hexadecane transport in Cd-/naphthalene-contaminated calcareous soils. In Fig. 6, high value of C/C_0 for n-hexadecane in OS, CS and NS were observed along with high flow velocity, which means the amount of n-hexadecane transport increased with the increasing flow velocity. Similar results had observed by some studies (Alazaiza et al., 2021; Alazaiza et al., 2020). In Table 3, it should be pointed out that the value of S_{max} decreased with high Darcy flow (0.69 cm/min) while the value of K_{att} was to be the minimum at Darcy flow of 0.12 cm/min. It suggested that smaller Darcy velocity may improve the irreversible retention but inhibit the reversible retention of n-hexadecane in calcareous soil samples. The mass recovery rate of

n-hexadecane transport increased when the set flow velocity reached 4 mL/min (Table 3), indicating the transport of n-hexadecane can be improved. Overall, n-hexadecane was more likely to break through CS/NS column with a high flow velocity.

Table 3 the parameters of fitted model

Column No.	Soil sample	Set flow (mL/min)	Darcy velocity (cm/min)	The mass recovery rate (%)	S_{max1} (mg/g) [a]	K_{att} (min^{-1}) [b]	R^2
1	OS	1	0.12	30.96	0.3384	0.0224	0.9711
2	OS	1	0.12	27.81	0.3896	0.0279	0.9401
3	OS	2	0.31	32.87	0.2855	0.0825	0.9827
4	OS	2	0.31	35.14	0.2639	0.0861	0.9429
5	OS	4	0.69	42.08	0.2368	0.0886	0.9818
6	OS	4	0.69	40.03	0.2100	0.0827	0.9598
7	CS	1	0.12	30.80	0.2512	0.0172	0.9719
8	CS	1	0.12	28.99	0.2368	0.0216	0.9768
9	CS	2	0.31	35.36	0.1639	0.0377	0.9771
10	CS	2	0.31	37.51	0.1468	0.0361	0.9524
11	CS	4	0.69	57.68	0.1270	0.0652	0.9429
12	CS	4	0.69	54.21	0.1011	0.0681	0.9577
13	NS	1	0.12	43.98	0.2377	0.0125	0.9681
14	NS	1	0.12	40.11	0.2033	0.0153	0.9767
15	NS	2	0.31	56.98	0.1309	0.0394	0.9888
16	NS	2	0.31	57.19	0.1214	0.0365	0.9459
17	NS	4	0.69	58.66	0.1160	0.0490	0.9695
18	NS	4	0.69	56.98	0.1270	0.0424	0.9872

[a] the maximum solid-phase retention capacity of n-hexadecane in attachment site.

[b] the attachment rate.

Effect of flow velocity on retention of n-hexadecane in the calcareous soil samples

As shown in Fig. 7, the maximum concentrations of n-hexadecane were retained in -12 cm, suggesting that n-hexadecane may be migrated downward by gravity force after leaching. The mass recovery rate of n-hexadecane effluent in CS/NS packed column was higher than in OS packed column (Table 3). Clearly, Cd/naphthalene reduced the retention content of n-hexadecane at various set flow velocity. Previous studies found that soil components such as SOM play an important role in retaining petroleum hydrocarbons (Adam et al., 2002; Cai et al., 2019). The DOM concentration of CS (313.10 mg/kg) was higher than that of OS (88.35 mg/kg) (Table S1), and the intensity of fulvic acid peak in CS was stronger than in OS (Fig. 3). It may be explained that the transport of hydrophobic substance was enhanced by increasing the concentration of fulvic acid (Dong et al., 2021; Sojitra et al., 1996; Yu et al., 2011). Moreover, batch experiments showed a higher n-hexadecane adsorption efficiency of NS than that of OS, since soil samples can expose additional attachment sites to n-hexadecane in shaking condition. However, adsorption sites are not available in column experiment, and the n-hexadecane transport may more affect by hydrodynamics (Wang et al., 2020b). In Fig. 7, when the flow velocity was 1 mL/min, the retention content of n-hexadecane in each soil column reached maximum. The effect of flow velocity on n-hexadecane retention is more pronounced at 4 mL/min. In Table 3, the mass recovery rate of n-hexadecane in effluent improved when flow velocity raised from 1 mL/min to 4 mL/min. Some studies also reported an increasing velocity result in an easier transport of contaminations in soil (Jiang et al., 2019; Yang et al., 2020). Macroscopically, the increasing flow velocity caused the decreasing residence of n-hexadecane in OS, CS and NS column, respectively.

Conclusion

This study provides valuable insights into the transport and retention of n-hexadecane in calcareous soil in karst areas. The results showed that the surface functional group and the mineralogical composition in calcareous soil did not change after Cd/naphthalene coating. Cd/naphthalene dramatically increased the adsorption efficiency of n-hexadecane on calcareous soil, but the function was limitation. The increasing pH value reduced the adsorption capacity in all groups due to the changed surface charges of soil samples and n-hexadecane. The higher transport efficiency and the lower retention efficiency of n-hexadecane in CS/NS depended on the more negative charge coating. Higher flow velocity is a key factor determining the fate of n-hexadecane in calcareous soils in karst areas. As a result, n-hexadecane is more likely to move far in cadmium-/naphthalene-contaminated calcareous soil with high flow velocity in karst areas and thereby impose serious risk to groundwater.

Declarations

Acknowledgments

This study was financially supported by the National Natural Science Foundation of China (No. 51668006) and the Innovation Project of Guangxi Graduate Education (No. YCSW2021015 and No. YCBZ2021016).

Statements & Declarations

Funding

This work was supported by the National Natural Science Foundation of China (No. 51668006) and the Innovation Project of Guangxi Graduate Education (No. YCSW2021015 and No. YCBZ2021016).

Competing interests

The authors have no relevant financial or non-financial interests to disclose.

Author contributions

All authors contributed to the study conception and design. All authors read and approved the final manuscript.

Yiting Huang: Methodology; Software; Investigation; Writing-Original Draft; Visualization; Project administration.

Yankui Tang: Conceptualization; Resources; Writing-Review & Editing; Supervision; Funding acquisition.

Yi Liang: Methodology; Investigation; Software; Editing.

Zhenze Xie: Methodology; Material preparation; Investigation.

Jipeng Wu: Data collection; Analysis.

Jiajie Huang: Data collection; Experiment.

Shanxiong Wei: Experiment; Editing.

Shaojiang Nie: Experiment; Software.

Tao Jiang: Experiment.

References

1. Adam, G., Gamoh, K., Morris, D.G., Duncan, H., 2002. Effect of alcohol addition on the movement of petroleum hydrocarbon fuels in soil. Science of The Total Environment, 286(1): 15–25.
2. Alazaiza, M.Y.D., Ramli, M.H., Copty, N.K., Ling, M.C., 2021. Assessing the impact of water infiltration on LNAPL mobilization in sand column using simplified image analysis method. Journal of

Contaminant Hydrology, 238: 103769.

3. Alazaiza, M.Y.D., Ramli, M.H., Copty, N.K., Sheng, T.J., Aburas, M.M., 2020. LNAPL saturation distribution under the influence of water table fluctuations using simplified image analysis method. Bulletin of Engineering Geology and the Environment, 79(3): 1543–1554.
4. Albert, H.A. et al., 2021. Influence of biochar and soil properties on soil and plant tissue concentrations of Cd and Pb: A meta-analysis. Science of The Total Environment, 755: 142582.
5. Brils, J.M. et al., 2002. Oil effect in freshly spiked marine sediment on Vibrio fischeri, Corophium volutator, and Echinocardium cordatum. Environ Toxicol Chem, 21(10): 2242–51.
6. Cai, T. et al., 2019. Effects of total organic carbon content and leaching water volume on migration behavior of polycyclic aromatic hydrocarbons in soils by column leaching tests. Environmental Pollution, 254: 112981.
7. Cai, Z. et al., 2017. Effects of oil dispersants on settling of marine sediment particles and particle-facilitated distribution and transport of oil components. Marine Pollution Bulletin, 114(1): 408–418.
8. Chen, W., Hou, L., Luo, X., Zhu, L., 2009. Effects of chemical oxidation on sorption and desorption of PAHs in typical Chinese soils. Environmental Pollution, 157(6): 1894–1903.
9. Delle Site, A., 2001. Factors Affecting Sorption of Organic Compounds in Natural Sorbent/Water Systems and Sorption Coefficients for Selected Pollutants. A Review. Journal of Physical and Chemical Reference Data, 30(1): 187–439.
10. Dong, S. et al., 2021. Transport characteristics of fragmental polyethylene glycol terephthalate (PET) microplastics in porous media under various chemical conditions. Chemosphere, 276: 130214.
11. Dror, I., Gerstl, Z., Prost, R., Yaron, B., 2002. Abiotic behavior of entrapped petroleum products in the subsurface during leaching. Chemosphere, 49(10): 1375–1388.
12. Fang, H. et al., 2015. Evidence of the adsorption of hydroxide ion at hexadecane/water interface from second harmonic generation study. RSC Advances, 5(30): 23578–23585.
13. Grządka, E., 2011. Competitive adsorption in the system: carboxymethylcellulose/surfactant/electrolyte/Al2O3. Cellulose, 18(2): 291–308.
14. Guo, Y., Wen, Z., Zhang, C., Jakada, H., 2020. Contamination and natural attenuation characteristics of petroleum hydrocarbons in a fractured karst aquifer, North China. Environmental Science and Pollution Research, 27(18): 22780–22794.
15. He, L., Li, X., Wu, G., Lin, F., Sui, H., 2013. Distribution of Saturates, Aromatics, Resins, and Asphaltenes Fractions in the Bituminous Layer of Athabasca Oil Sands. Energy & Fuels, 27(8): 4677–4683.
16. Jampasri, K., Pokethitiyook, P., Kruatrachue, M., Ounjai, P., Kumsopa, A., 2016. Phytoremediation of fuel oil and lead co-contaminated soil by Chromolaena odorata in association with Micrococcus luteus. International Journal of Phytoremediation, 18(10): 994–1001.
17. Jiang, X. et al., 2019. Transport and retention of phosphorus in soil with addition of Mg-Al layered double hydroxides: Effects of material dosage, flow velocity and pH. Chemical Engineering Journal,

378: 122154.

18. Jiang, Y.F., Sun, H., Yves, U.J., Li, H., Hu, X.F., 2016. Impact of biochar produced from post-harvest residue on the adsorption behavior of diesel oil on loess soil. Environmental Geochemistry and Health, 38(1): 243–253.
19. Khudur, L.S. et al., 2018. Implications of co-contamination with aged heavy metals and total petroleum hydrocarbons on natural attenuation and ecotoxicity in Australian soils. Environmental Pollution, 243: 94–102.
20. Kicińska, A., Pomykała, R., Izquierdo-Diaz, M., 2022. Changes in soil pH and mobility of heavy metals in contaminated soils. European Journal of Soil Science, 73(1): e13203.
21. Kim, H.-J., Phenrat, T., Tilton, R.D., Lowry, G.V., 2012. Effect of kaolinite, silica fines and pH on transport of polymer-modified zero valent iron nano-particles in heterogeneous porous media. Journal of Colloid and Interface Science, 370(1): 1–10.
22. Lü, W. et al., 2020. Characteristics and influencing factors of hydrochemistry and dissolved organic matter in typical karst water system. Environmental Science and Pollution Research, 27(10): 11174–11183.
23. Li, J. et al., 2021. Polycyclic aromatic hydrocarbon and n-alkane pollution characteristics and structural and functional perturbations to the microbial community: a case-study of historically petroleum-contaminated soil. Environmental Science and Pollution Research, 28(9): 10589–10602.
24. Li, X. et al., 2012. Operational Parameters, Evaluation Methods, And Fundamental Mechanisms: Aspects of Nonaqueous Extraction of Bitumen from Oil Sands. Energy & Fuels, 26(6): 3553–3563.
25. Li, Y., Bhushan, B., 2015. The effect of surface charge on the boundary slip of various oleophilic/phobic surfaces immersed in liquids. Soft Matter, 11(38): 7680–7695.
26. Lu, R. et al., 2013. Characterizing the interactions between polycyclic aromatic hydrocarbons and fulvic acids in water. Environmental Science and Pollution Research, 20(4): 2220–2225.
27. Luo, X. et al., 2022. Particulate organic carbon exports from the terrestrial biosphere controlled by erosion. CATENA, 209: 105815.
28. Nguyen, X.P. et al., 2013. Effects of pore water chemical composition on the hydro-mechanical behavior of natural stiff clays. Engineering Geology, 166: 52–64.
29. Ossai, I.C., Ahmed, A., Hassan, A., Hamid, F.S., 2020. Remediation of soil and water contaminated with petroleum hydrocarbon: A review. Environmental Technology & Innovation, 17: 100526.
30. Peng, Y. et al., 2022. Hydrochemical environment of a fractured karst aquifer influenced by petroleum hydrocarbons. Environmental Science and Pollution Research, 29(2): 2244–2257.
31. Pradubmook, T., O'Haver, J.H., Malakul, P., Harwell, J.H., 2003. Effect of pH on adsolubilization of toluene and acetophenone into adsorbed surfactant on precipitated silica. Colloids and Surfaces A: Physicochemical and Engineering Aspects, 224(1): 93–98.
32. Rosales, R.M., Martínez-Pagán, P., Faz, A., Bech, J., 2014. Study of subsoil in former petrol stations in SE of Spain: Physicochemical characterization and hydrocarbon contamination assessment.

Journal of Geochemical Exploration, 147: 306–320.

33. Saeedi, M., Li, L.Y., Grace, J.R., 2018. Effect of organic matter and selected heavy metals on sorption of acenaphthene, fluorene and fluoranthene onto various clays and clay minerals. Environmental Earth Sciences, 77(8): 305.
34. Samaei, M.R. et al., 2020. Isolation and Kinetic Modeling of New Culture from Compost with High Capability of Degrading n-Hexadecane, Focused on Ochrobactrum Oryzae and Paenibacillus Lautus. Soil and Sediment Contamination: An International Journal, 29(4): 384–396.
35. Samaei, M.R. et al., 2022. Investigating the effects of combined bio-enhancement and bio-stimulation on the cleaning of hexadecane-contaminated soils. Journal of Environmental Chemical Engineering, 10(1): 106914.
36. Schwarz, K., Gocht, T., Grathwohl, P., 2011. Transport of polycyclic aromatic hydrocarbons in highly vulnerable karst systems. Environmental Pollution, 159(1): 133–139.
37. Simunek, J., Genuchten, M., Sejna, M., 1999. The HYDRUS-1D software package for simulating the one-dimensional movement of water, heat, and multiple solutes in variably-saturated media.
38. Sojitra, I., Valsaraj, K.T., Reible, D.D., Thibodeaux, L.J., 1996. Transport of hydrophobic organics by colloids through porous media 2. Commercial humic acid macromolecules and polyaromatic hydrocarbons. Colloids and Surfaces A: Physicochemical and Engineering Aspects, 110(2): 141–157.
39. Song, J.E. et al., 2011. Hydrophobic Interactions Increase Attachment of Gum Arabic- and PVP-Coated Ag Nanoparticles to Hydrophobic Surfaces. Environmental Science & Technology, 45(14): 5988–5995.
40. Steliga, T., Kluk, D., 2020. Application of Festuca arundinacea in phytoremediation of soils contaminated with Pb, Ni, Cd and petroleum hydrocarbons. Ecotoxicology and Environmental Safety, 194: 110409.
41. Sun, Y. et al., 2019. Vertical migration from surface soils to groundwater and source appointment of polycyclic aromatic hydrocarbons in epikarst spring systems, southwest China. Chemosphere, 230: 616–627.
42. Wang, F. et al., 2017. Effects of humic acid and heavy metals on the sorption of polar and apolar organic pollutants onto biochars. Environmental Pollution, 231: 229–236.
43. Wang, P. et al., 2020a. Effects of exogenous dissolved organic matter on the adsorption–desorption behaviors and bioavailabilities of Cd and Hg in a plant–soil system. Science of The Total Environment, 728: 138252.
44. Wang, Y. et al., 2020b. Factors affecting the transport of petroleum colloids in saturated porous media. Colloids and Surfaces A: Physicochemical and Engineering Aspects, 585: 124134.
45. Wen, Y., Li, W., Yang, Z., Zhang, Q., Ji, J., 2020. Enrichment and source identification of Cd and other heavy metals in soils with high geochemical background in the karst region, Southwestern China. Chemosphere, 245: 125620.

46. Wu, G., He, L., Chen, D., 2013. Sorption and distribution of asphaltene, resin, aromatic and saturate fractions of heavy crude oil on quartz surface: Molecular dynamic simulation. Chemosphere, 92(11): 1465–1471.
47. Wu, M. et al., 2017. Bacterial community shift and hydrocarbon transformation during bioremediation of short-term petroleum-contaminated soil. Environmental Pollution, 223: 657–664.
48. Wu, X. et al., 2020. Transport of polystyrene nanoplastics in natural soils: Effect of soil properties, ionic strength and cation type. Science of The Total Environment, 707: 136065.
49. Xu, G. et al., 2022. Vertical distribution characteristics and interactions of polycyclic aromatic compounds and bacterial communities in contaminated soil in oil storage tank areas. Chemosphere, 301: 134695.
50. Xu, Z. et al., 2020. Selective adsorption of PHC and regeneration of washing effluents by modified diatomite. Water Science and Technology, 81(10): 2066–2077.
51. Yan, L. et al., 2019. Effect of swine biogas slurry application on soil dissolved organic matter (DOM) content and fluorescence characteristics. Ecotoxicology and Environmental Safety, 184: 109616.
52. Yang, J.-y. et al., 2020. Adsorption-desorption and co-migration of vanadium on colloidal kaolinite. Environmental Science and Pollution Research, 27(15): 17910–17922.
53. Yang, J., Chen, H., Nie, Y., Wang, K., 2019. Dynamic variations in profile soil water on karst hillslopes in Southwest China. CATENA, 172: 655–663.
54. Yang, M., Yang, Y.S., Du, X., Cao, Y., Lei, Y., 2013. Fate and Transport of Petroleum Hydrocarbons in Vadose Zone: Compound-specific Natural Attenuation. Water, Air, & Soil Pollution, 224(3): 1439.
55. Yang, W. et al., 2017a. Antagonistic effect of humic acid and naphthalene on biochar colloid transport in saturated porous media. Chemosphere, 189: 556–564.
56. Yang, W. et al., 2017b. Effect of naphthalene on transport and retention of biochar colloids through saturated porous media. Colloids and Surfaces A: Physicochemical and Engineering Aspects, 530: 146–154.
57. Yang, Y., Ratté, D., Smets, B.F., Pignatello, J.J., Grasso, D., 2001. Mobilization of soil organic matter by complexing agents and implications for polycyclic aromatic hydrocarbon desorption. Chemosphere, 43(8): 1013–1021.
58. Yu, H., Huang, G.-h., An, C.-j., Wei, J., 2011. Combined effects of DOM extracted from site soil/compost and biosurfactant on the sorption and desorption of PAHs in a soil–water system. Journal of Hazardous Materials, 190(1): 883–890.
59. Zeng, J. et al., 2020. Determining rainwater chemistry to reveal alkaline rain trend in Southwest China: Evidence from a frequent-rainy karst area with extensive agricultural production. Environmental Pollution, 266: 115166.
60. Zhang, L. et al., 2012. Transport of Fullerene Nanoparticles (nC60) in Saturated Sand and Sandy Soil: Controlling Factors and Modeling. Environmental Science & Technology, 46(13): 7230–7238.

61. Zhao, Y. et al., 2017. Bioremediation of Cd by strain GZ-22 isolated from mine soil based on biosorption and microbially induced carbonate precipitation. Environmental Science and Pollution Research, 24(1): 372–380.
62. Zheng, R. et al., 2016. Land Use Effects on the Distribution and Speciation of Heavy Metals and Arsenic in Coastal Soils on Chongming Island in the Yangtze River Estuary, China. Pedosphere, 26(1): 74–84.
63. Zhou, H. et al., 2019. Fungal proliferation and hydrocarbon removal during biostimulation of oily sludge with high total petroleum hydrocarbon. Environmental Science and Pollution Research, 26(32): 33192–33201.

Figures

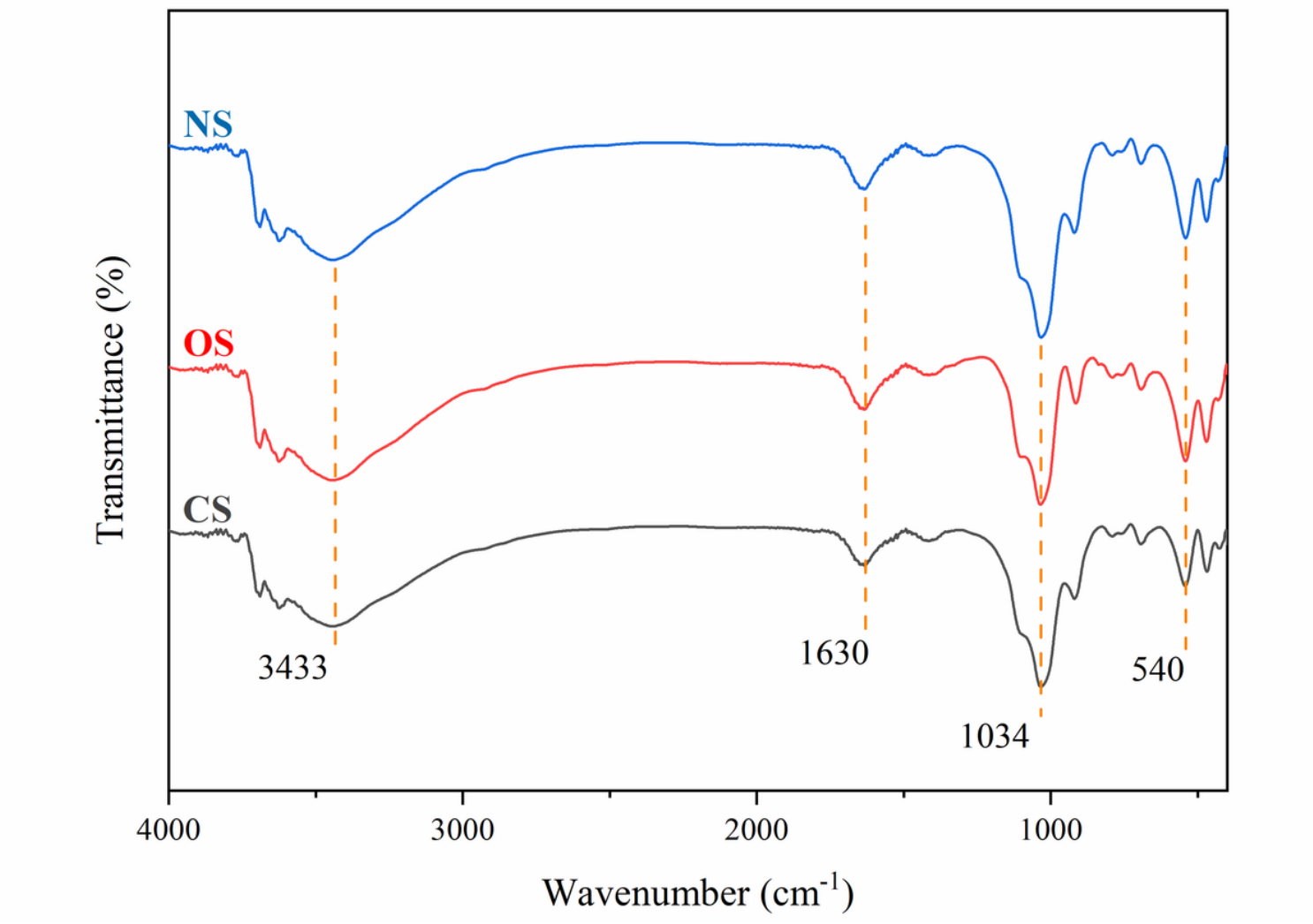

Figure 1

FTIR spectrum of OS, CS and NS

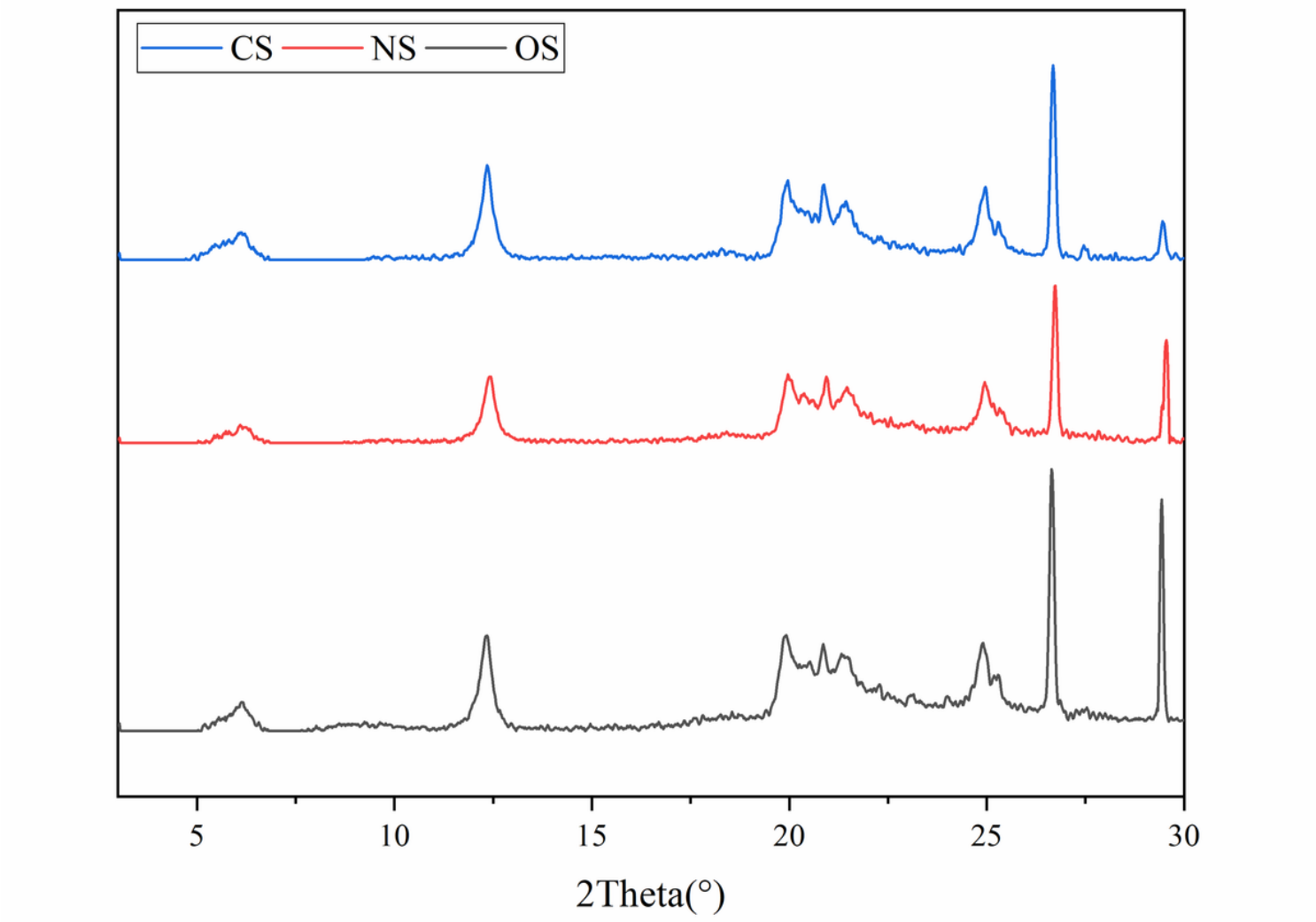

Figure 2

XRD pattern of OS, CS and NS

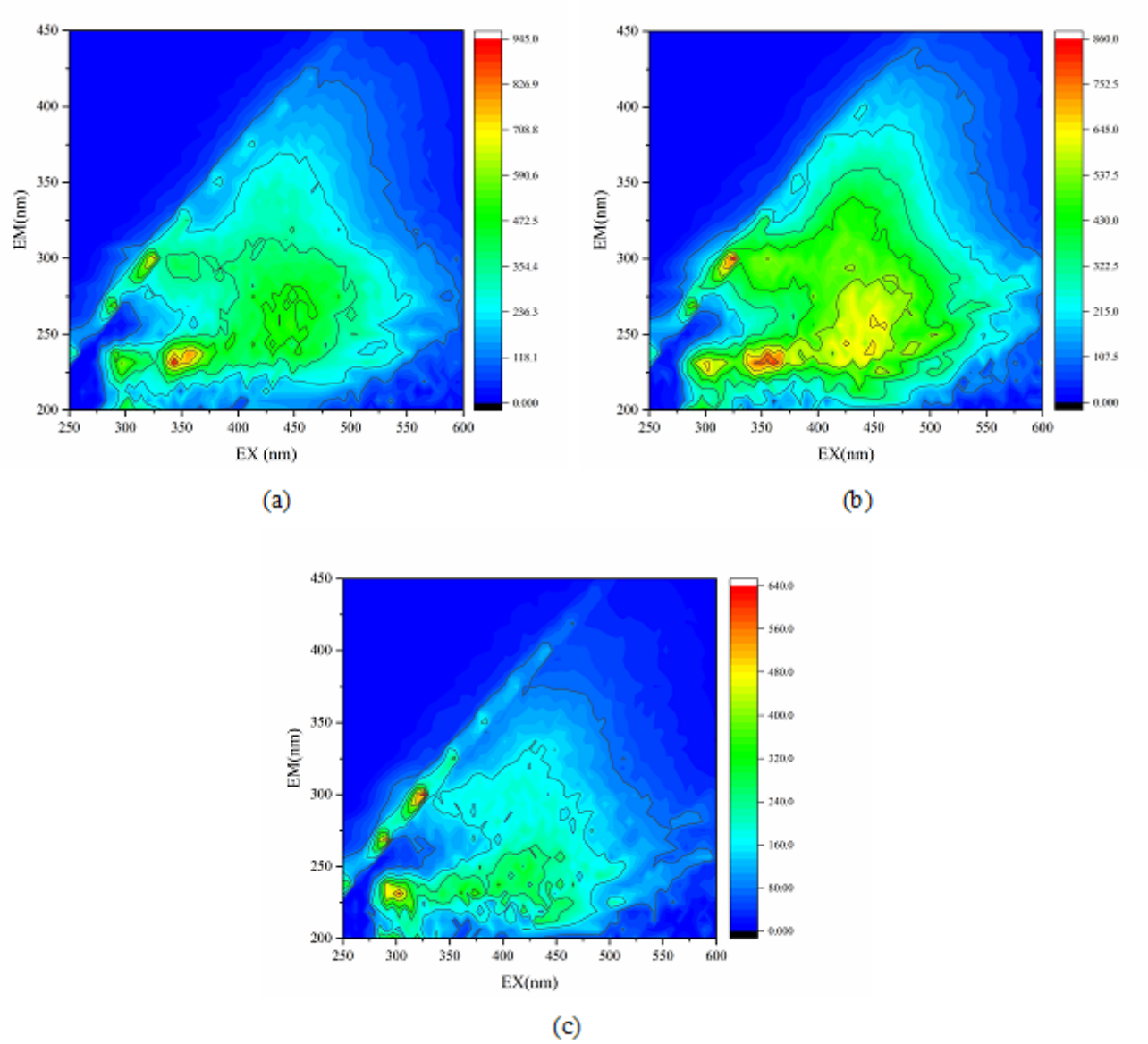

Figure 3

Fluorescence spectra of (a) OS, (b) CS and (c) NS

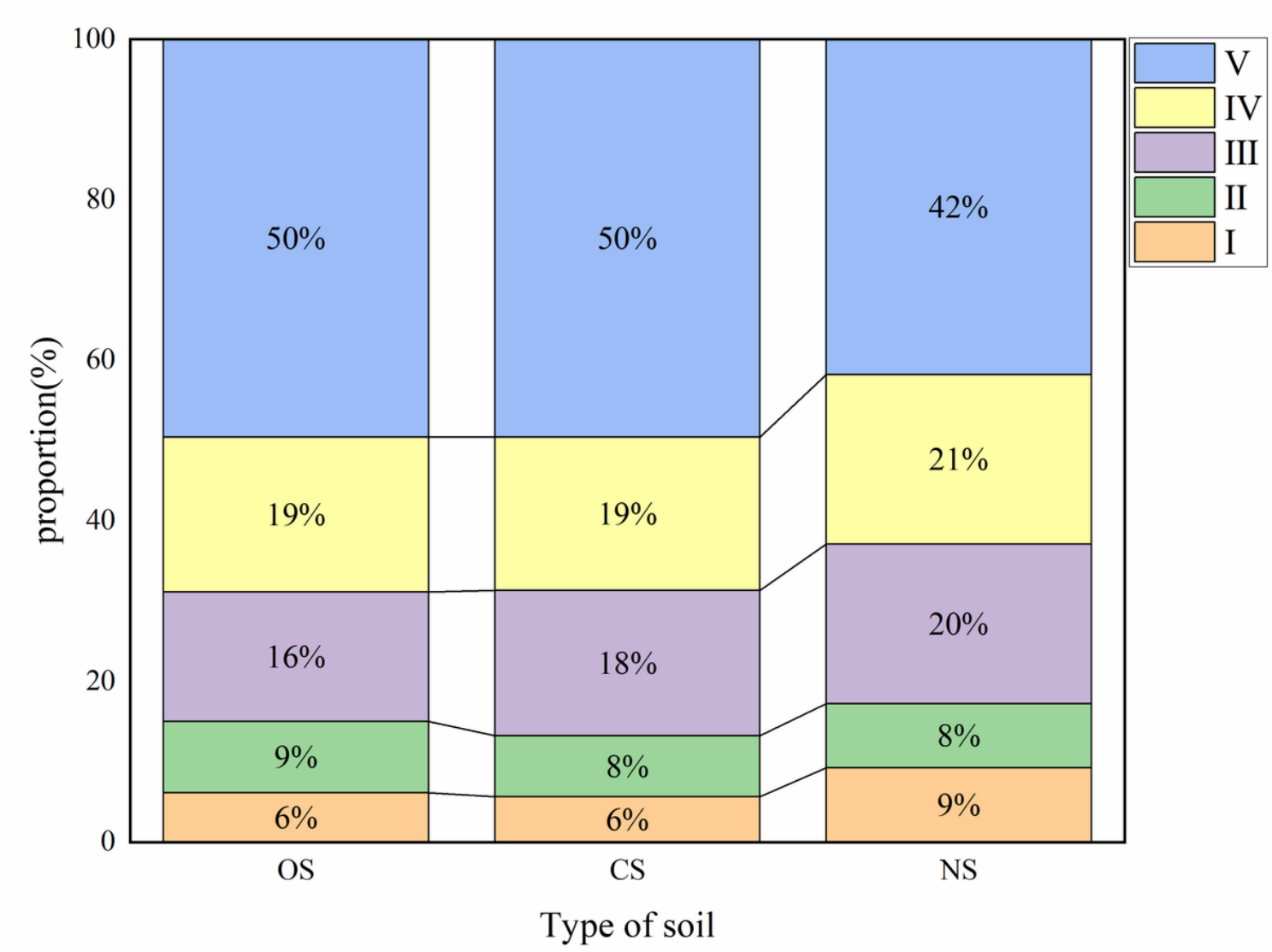

Figure 4

Fluorescence components of DOM in OS, CS and NS. . Aromatic protein, . Aromatic protein, . Fulvic acid-like, . Soluble microbial by-product-like, . Humic acid-like

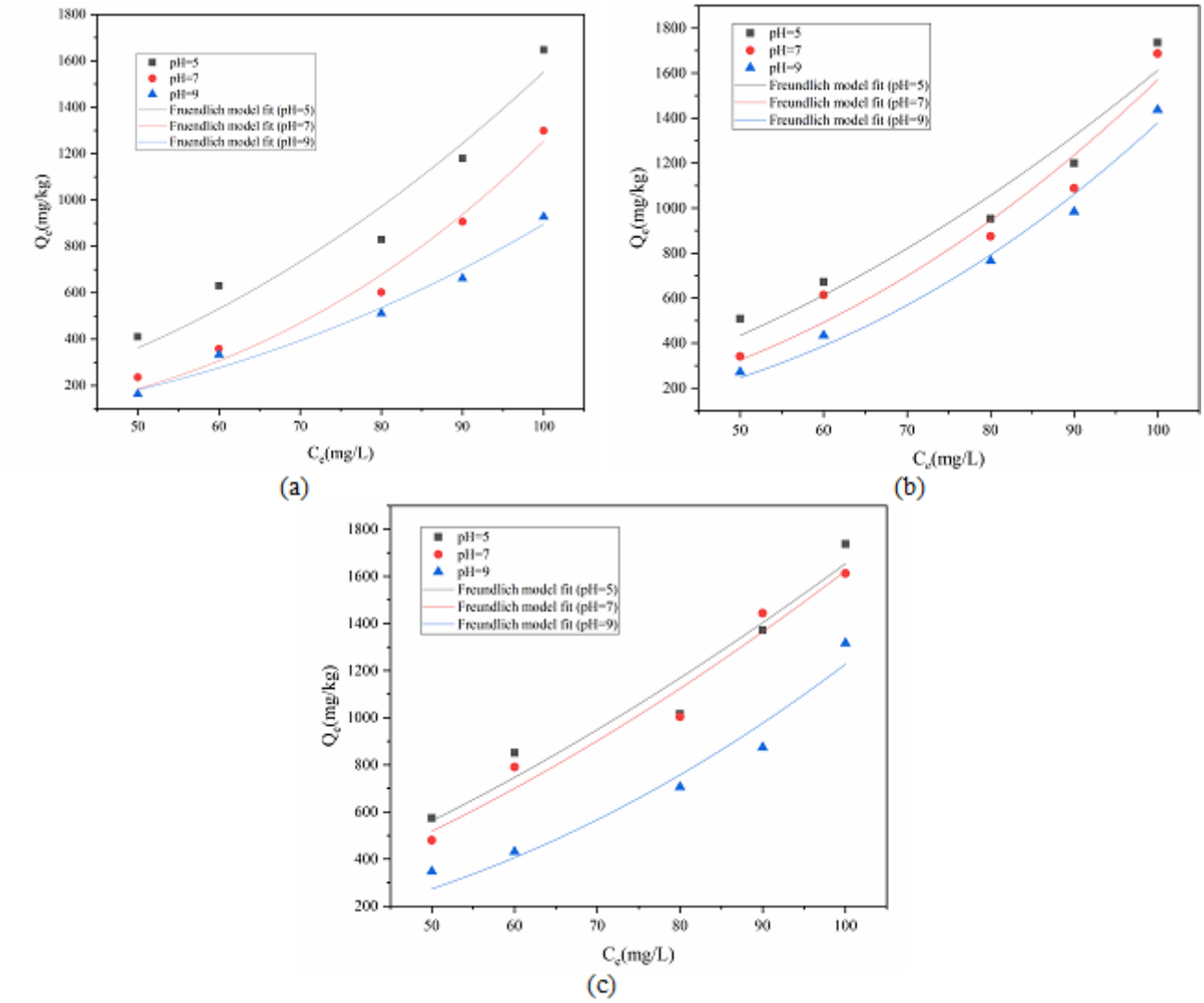

Figure 5

Adsorption isotherm of n-hexadecane on (a) OS, (b) CS and (c) NS with various pH (5, 7, 9) fitted by Freundlich model. The ratio of soil sample and n-hexadecane solution was 1:50. The various concentration of n-hexadecane were set 50, 60, 80, 90 and 100 mg/L. Adsorption time was set 4 h (140 rpm, 25±1 °C). Q_e is the amount of n-hexadecane adsorbed by soil samples. C_e is the concentration of n-hexadecane

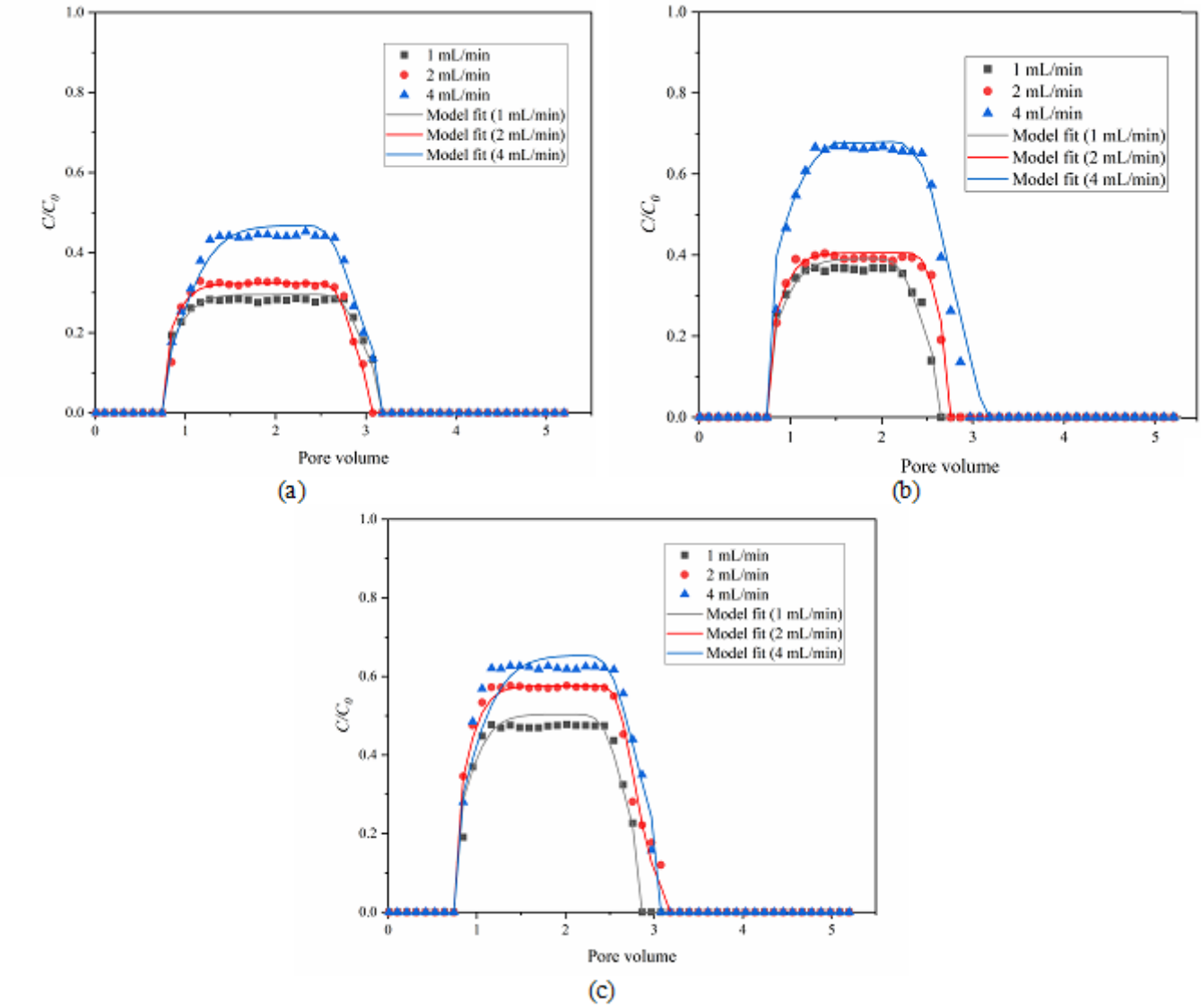

Figure 6

The breakthrough curves of n-hexadecane in (a) OS, (b) CS and (c) NS with the set flow velocity of 1, 2, and 4 mL/min. The influent concentration of n-hexadecane was set 100 mg/L. C/C_0 is normalized effluent concentration, where C and C_0 were the concertation of n-hexadecane in the effluents and influents, respectively

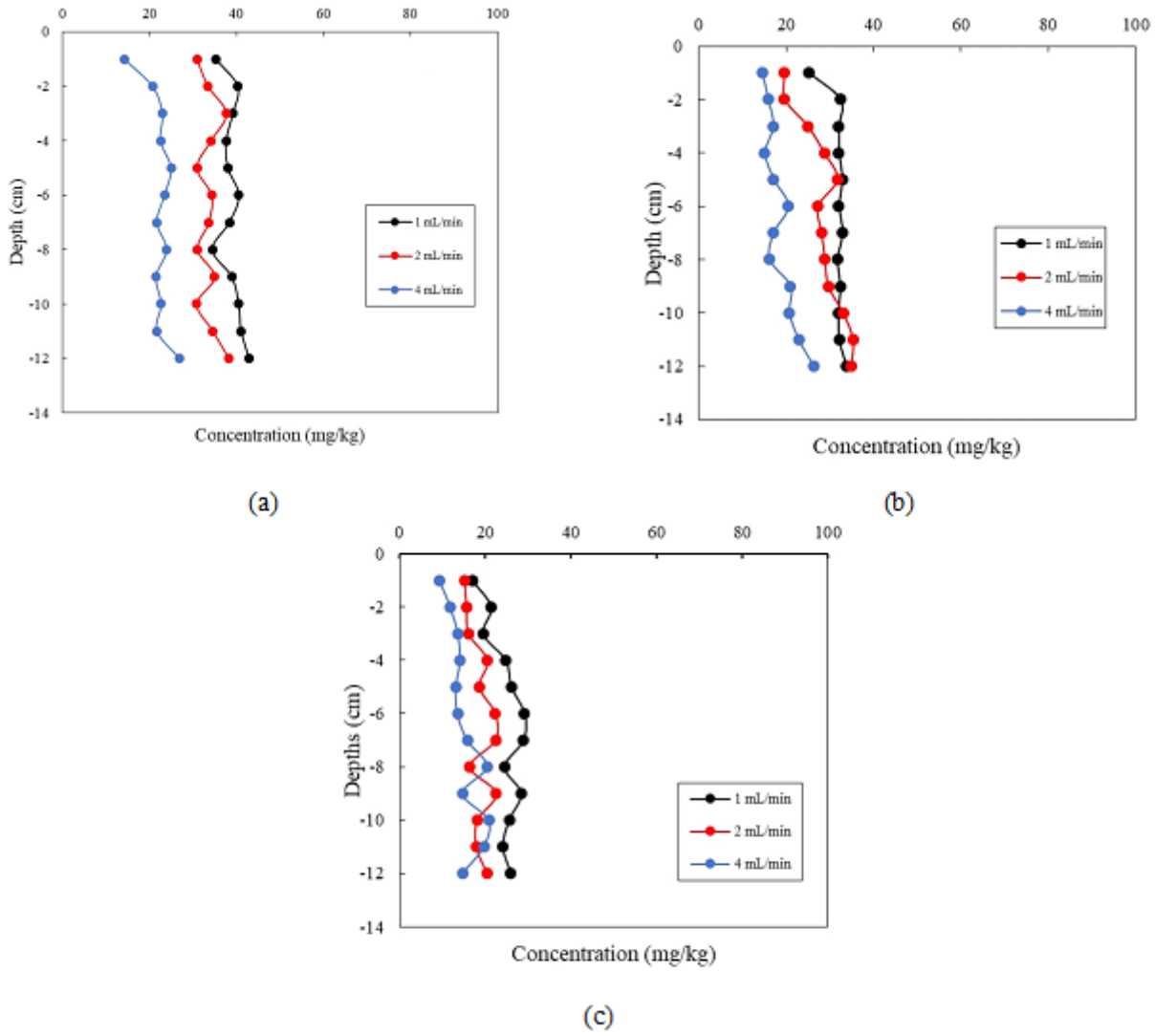

Figure 7

Retention profiles of n-hexadecane in (a) OS, (b) CS and (c) NS column under different flow velocity1, 2, and 4 mL/min. The influent concentration of n-hexadecane was set 100 mg/L

Supplementary Files

This is a list of supplementary files associated with this preprint. Click to download.

- Supplementartmaterials.doc
- Supplementartmaterialsamendment.doc